Self-similar evolutions of parabolic, Hermite-Gaussian, and hybrid optical pulses: Universality and diversity

Shihua Chen,[1,*] Lin Yi,[1,2] Dong-Sheng Guo,[2,3,†] and Peixiang Lu[2]
[1]*Department of Physics, Huazhong University of Science and Technology, Wuhan 430074, China*
[2]*State Key Laboratory of Laser Technology, Huazhong University of Science and Technology, Wuhan 430074, China*
[3]*Department of Physics, Southern University, Baton Rouge, Louisiana 70813, USA*
(Received 17 March 2005; published 26 July 2005)

Three novel types of self-similar solutions, termed parabolic, Hermite-Gaussian, and hybrid pulses, of the generalized nonlinear Schrödinger equation with varying dispersion, nonlinearity, and gain or absorption are obtained. The properties of the self-similar evolutions in various nonlinear media are confirmed by numerical simulations. Despite the diversity of their formations, these self-similar pulses exhibit many universal features which can facilitate significantly the achievement of well-defined linearly chirped output pulses from an optical fiber, an amplifier, or an absorption medium, under certain parametric conditions. The other intrinsic characteristics of each type of self-similar pulses are also discussed.

DOI: 10.1103/PhysRevE.72.016622 PACS number(s): 42.65.Re, 42.81.Dp, 47.20.Ky, 42.65.Sf

Self-similarity has been intensively explored in many areas of physics such as hydrodynamics and quantum field theory [1]. Also in nonlinear optics, there has been a significant surge of research activities on self-similarity. As examples, the self-similar behaviors in stimulated Raman scattering [2], the evolution of self-written waveguides [3], the formation of Cantor set fractals in materials that support spatial solitons [4], the evolution of optical wave collapse [5], and the nonlinear propagation of parabolic pulses in optical fibers with normal dispersion [6] were investigated. Recent attention has been riveted on the self-similar propagation of parabolic optical pulses in an optical fiber amplifier [7], a dispersion-decreasing optical fiber [8], and a laser resonator [9], opening prospects for studying the self-similar phenomena in dispersion and nonlinearity management systems.

It is of interest to note that the system described by the generalized nonlinear Schrödinger (NLS) equation with varying coefficients can lead to exact sech- and tanh-shaped self-similar pulses [10]. These pulses are confirmed to coincide with the solitary wave or soliton solutions presented by Serkin and Hasegawa [11]. As reported, these solitonlike pulses possess a strictly linear chirp and have potential applications in many fields of current optical technology. It is also noteworthy that in Ref. [12] exact self-similar solutions accompanied with a controllable pulse position and a nonlinear chirp were found in a similar fashion, a substantial extension to the results drawn in Refs. [10,11] by considering the nonlinear gain into the generalized NLS equation model.

In this paper, we present the discovery of three types of self-similar solutions, other than those with sech or tanh profiles [10,11], to this generalized NLS equation with varying coefficients. For convenience, we term them parabolic, Hermite-Gaussian (HG), and hybrid pulse solutions for their characteristic pulse profiles. Despite the diversity of their formations, these pulses exhibit many universal features such as self-similarity in shape, enhanced linearity in chirp, controllability of pulse position, stability against perturbations, and resistance to optical wave breaking [6,8], suggesting potential applications in ultrashort pulse generation and optical fiber communications. In addition, the valid parametric ranges for and the intrinsic characteristics of each type of self-similar pulses are also investigated in detail. As examples, a parabolic pulse always forms in the normal dispersion regime for usual posivitely nonlinear materials and has no direct concern with the initial pulse shape, while HG and hybrid pulses can be generated in both the normal and anomalous dispersion regimes, and are dependent upon the specific initial shapes; a parabolic pulse continues to be temporally broadened during propagation, while the latter two may experience an initial pulse narrowing stage under certain initial conditions. As for HG and hybrid pulses, there also exist some obvious discrepancies between them which deserve extra attention, e.g., HG pulses result from the predominant dispersion over weak nonlinearity, while hybrid pulses are attributed to the strong interplay between dispersion and nonlinearity. All these features are found for the first time and would find widespread applications in optics and other nonlinear sciences such as Bose-Einstein condensates.

For our studies, the generalized NLS equation with varying coefficients is expressed as [10,11]

$$i\psi_z = \frac{\beta(z)}{2}\psi_{\tau\tau} - \gamma(z)|\psi|^2\psi + i\frac{g(z)}{2}\psi, \tag{1}$$

where $\psi(z,\tau)$ is the complex envelope of the electric field in a comoving frame, z is the propagation distance, τ is the retarded time, $\beta(z)$ is the group velocity dispersion (GVD) parameter, $\gamma(z)$ is the nonlinearity parameter, and $g(z)$ is the distributed gain function. The subscripts z and τ denote the spatial and temporal partial derivatives. It is of note that this model equation (1) has exact sech-shaped $[\rho(z)<0]$ and tanh-shaped $[\rho(z)>0]$ self-similar solutions, where $\rho(z)=\beta(z)/\gamma(z)$ [10,11]. But here we are concerned with other

*Electronic address: cshua@mail.edu.cn
†Electronic address: dsguo@grant.phys.subr.edu

novel types of self-similar solutions than these solitonlike solutions.

To this end, we introduce a z-dependent variable D through $D(z)=\int_0^z \beta(z')dz'$, and define the complex field as $\psi(z,\tau)=A(z,\tau)\exp[i\Phi(z,\tau)]$, where A and Φ are real functions of z and τ. With this variable and after a little algebra, we can transform Eq. (1) into

$$A_D = A_\tau \Phi_\tau + \frac{1}{2}A\Phi_{\tau\tau} + \frac{1}{2}\frac{g(z)}{\beta(z)}A, \tag{2}$$

$$A\Phi_D = \frac{1}{2}(A\Phi_\tau^2 - A_{\tau\tau}) + \frac{1}{\rho(z)}A^3. \tag{3}$$

Then two quantities $T(z)$ and $E(z)=E_0\exp[\int_0^z g(z')dz']$ are introduced, where E_0 is the energy of incident pulse. In terms of these quantities, the amplitude $A(z,\tau)$ is further scaled as

$$A(z,\tau) = \sqrt{\frac{\kappa E(z)}{T(z)}}F(\theta), \tag{4}$$

where $\theta(z,\tau)$ is the self-similarity variable and κ is a positive constant. Furthermore, the phase of the complex field is assumed to be [12]

$$\Phi(z,\tau) = a(z) + b(z)[\tau - \tau_c(z)] + c(z)[\tau - \tau_c(z)]^2, \tag{5}$$

where $\tau_c(z)$ denotes the pulse position. In this quadratic form, $a(z)$ is the phase offset, while the partial derivative $\delta\omega(\tau)=-\partial\Phi(z,\tau)/\partial\tau$ accounts for the linear chirp [7]. As a consequence, Eq. (2) yields

$$\theta = \frac{\tau - \tau_c(z)}{T(z)}, \quad b(z) = -\frac{d}{dD}\tau_c(z), \tag{6}$$

$$c(z) = -\frac{1}{2}\frac{d}{dD}\ln[T(z)]. \tag{7}$$

Note that the phase parameter $b(z)$ remains invariant on propagation, i.e., $b(z)=b_0$, and therefore the pulse position $\tau_c(z)$ is given by $\tau_c(z)=\tau_0-b_0D$. Furthermore, it is found that Eqs. (6) and (7) are universally applicable for all types of self-similar pulses. Here and in what follows, the symbols containing subscript "0" are used to represent the initial values of the corresponding parameters at distance $z=0$.

By means of Eqs. (4)–(7), a nonlinear differential equation for $F(\theta)$ is readily derived from Eq. (3),

$$\eta - \mu\theta^2 + \nu\frac{F''}{F} = F^2, \tag{8}$$

where the prime denotes the derivative relative to the variable θ and the coefficients η, μ, and ν are given by

$$\eta = \frac{T(z)\rho(z)}{\kappa E(z)}\left(\frac{da(z)}{dD} + \frac{1}{2}b_0^2\right), \tag{9}$$

$$\mu = \frac{1}{2\kappa}\frac{T^2(z)\rho(z)}{E(z)}\frac{d^2}{dD^2}T(z), \quad \nu = \frac{1}{2\kappa}\frac{\rho(z)}{E(z)T(z)}. \tag{10}$$

We note that by solving Eq. (8), many types of nontrivial self-similar solutions can be obtained, subject to the relative sizes of coefficients η, μ, and ν. As a typical example, when $\eta=-\lambda\rho_0/2\kappa E_0$, $\mu=0$, and $\nu=\rho_0/2\kappa E_0$, and according to the values of parameters λ and ρ_0, one can obtain easily the exact solitary wave and cnoidal wave solutions to Eq. (1) under the parametric condition $\rho(z)/E(z)=\rho_0 T(z)/E_0$, where $T(z)=1-2c_0D$ [10].

Now, we proceed to search for the self-similar solutions of Eq. (1) in the asymptotic limit. From Eq. (10) it is easily concluded that the coefficient ν vanishes when

$$\frac{\rho(z)}{E(z)} \to 0 \quad (\text{as } z \to \infty). \tag{11}$$

This parametric condition can be easily satisfied in a gain medium [7] or in dispersion-decreasing optical fibers [8]. Accordingly, by setting $\eta=1$, $\mu=1$, and $\kappa=3/4$, we obtain a parabolic solution of the amplitude

$$A(z,\tau) = \left\{\frac{3}{4}\frac{E(z)}{T(z)}\left[1 - \left(\frac{\tau - \tau_c(z)}{T(z)}\right)^2\right]\right\}^{1/2},$$

$$|\tau - \tau_c(z)| \leqslant T(z), \tag{12}$$

with $A(z,\tau)=0$ for $|\tau-\tau_c(z)|>T(z)$, where the pulse width $T(z)$ satisfies

$$T^2(z)\frac{d^2}{dD^2}T(z) = \frac{3E(z)}{2\rho(z)}, \tag{13}$$

which reveals the unique relation among $T(z)$, E_0, and the fiber parameters. As such, the phase offset $a(z)$ can be determined by

$$a(z) = a_0 - \frac{1}{2}b_0^2 D + \frac{3}{4}\int_0^z \frac{E(z')\gamma(z')}{T(z')}dz'. \tag{14}$$

In particular, from Eq. (7) we show that the linear chirp relates to the parameter $\beta(z)$ to a great extent. It indicates that the chirp is highly linearized as the pulse propagates in dispersion-decreasing optical fibers, but less linearized in dispersion-increasing optical fibers. This has important physical implications in achieving highly chirped or asymptotically chirp-free pulses.

A close inspection of Eq. (12) shows that for given fiber parameters, the evolution of a parabolic pulse, accompanied by a controllable pulse position $t_c(z)$, is determined only by the incident pulse energy, with the initial pulse shape determining only the "time" toward this asymptotic solution. We show also that the pulse energy is $E(z)=\int_{-\infty}^{\infty}|\psi(z,\tau)|^2 d\tau$, depending only on the gain profile. If $g(z)=0$, the energy is identical to its initial value E_0. It means that the parabolic pulse can propagate without radiating dispersive waves [6,8]. We show further that such a solution always exists under the condition $\rho(z)>0$. If $\rho(z)<0$, the GVD effect acts contrary to the nonlinearity induced self-phase modulation, leading to the pulse contractions or solitary waves, and therefore no obvious parabolic pulses can occur.

It should be emphasized that our parabolic solution (12) with wide-range condition (11) is a natural but significant generalization of the results reported in Refs. [6–8]. As seen, our solution provides a unified explanation of these previous

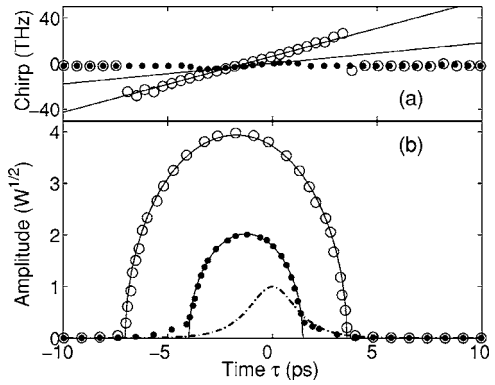

FIG. 1. Evolution of output pulse chirp (a) and amplitude (b) at $z=100$ m (solid circles) and 200 m (open circles) for an initial pulse $\psi(0,\tau)=\mathrm{sech}(\tau)\exp(i2\tau)$ (dash-dotted line), compared with the analytical results (solid line). The model parameters in Eq. (1) are given by $\beta(z)=\beta_0\exp(-0.01z)$, $\gamma(z)=\gamma_0\exp(0.01z)$, and $g(z)=g_0$, where $\beta_0=0.01$ ps^2 m^{-1}, $\gamma_0=0.01$ W^{-1} m^{-1}, and $g_0=0.02$ m^{-1}.

predictions for parabolic pulses, ranging from the constant dispersion optical fibers [6] to the dispersion-decreasing optical fibers [8]. In addition, another intriguing phenomenon that the dispersion-increasing fibers support parabolic pulses with arranged compensation (high gain or fast increasing nonlinearity) is also predictable and may result in an impact on theory and applications.

These theoretical predictions have been confirmed by numerical simulations of the underlying equation (1) using the split-step Fourier code [13]. Figure 1 shows the output pulse characteristics of chirp and amplitude at $z=100$ m (solid circles) and 200 m (open circles) for an initial pulse $\psi(0,\tau)=\mathrm{sech}(\tau)\exp(i2\tau)$ (dash-dotted line) in a dispersion-decreasing optical fiber amplifier, indicating the excellent agreement with our analytical results (solid line). It is also shown in Fig. 1(a) that the chirp is well linearized across the entire pulse width, and the slope $2|c(z)|$ increases with the distance of propagation. Nevertheless, owing to the enhanced interference between the leading and trailing regions of an optical pulse, such a parabolic evolution will be seriously spoiled after propagating a large enough distance, which in turn limits the increase of this slope.

On the other hand, if the parametric condition (11) approaches other extremes as $z\to\infty$, i.e.,

$$\frac{\rho(z)}{E(z)}\to\pm\infty, \tag{15}$$

then the term on the right-hand side of Eq. (8) can be neglected in the asymptotic limit. It is obvious that the condition (15) holds true in an absorption medium or in nonlinearity-decreasing fibers. Then by taking

$$T(z)=\left(\alpha+\frac{(D+\Delta)^2}{\alpha}\right)^{1/2}, \tag{16}$$

$$a(z)=a_0+\phi\left[\arctan\left(\frac{D+\Delta}{\alpha}\right)-\arctan\left(\frac{\Delta}{\alpha}\right)\right]-\frac{1}{2}b_0^2D, \tag{17}$$

we obtain the HG self-similar solutions of the amplitude

$$A(z,\tau)=\sqrt{\frac{\kappa E(z)}{T(z)}}\exp\left(-\frac{1}{2}\theta^2\right)H_n(\theta), \tag{18}$$

where $\kappa=(2^n n!\sqrt{\pi})^{-1}$ with non-negative integers n, $\phi=n+1/2$, $E(z)$ is the pulse energy, $T(z)$ goes by the general name of pulse width, θ is given by Eq. (6), and $H_n(\theta)$ are the Hermite polynomials of nth degree [14]. The parameters α and Δ in Eqs. (16)–(18) are given by

$$\alpha=\frac{T_0^2}{1+4c_0^2T_0^4},\quad \Delta=-\frac{2c_0T_0^4}{1+4c_0^2T_0^4}. \tag{19}$$

As can be seen, by setting $n=0$, Eq. (18) reduces to the fundamental Gaussian form

$$A(z,\tau)=\frac{1}{\pi^{1/4}}\sqrt{\frac{E(z)}{T(z)}}\exp\left[-\frac{1}{2}\left(\frac{\tau-\tau_c(z)}{T(z)}\right)^2\right]. \tag{20}$$

Notice that our HG solutions (18), as the name implies, are well characterized by both the Gaussian function and Hermite polynomials, and therefore exhibit even or odd symmetry when the index n is even or odd, respectively. Moreover, with the condition $c_0\,\mathrm{sgn}(D)>0$, these self-similar pulses can be drastically compressed when propagating toward the location $z_{\min}$ at which $D(z_{\min})=-\Delta$ and then be broadened after passing that point. We find further that the linear chirp for HG pulses evolves independently according to

$$c(z)=-\frac{1}{2}\frac{D+\Delta}{\alpha^2+(D+\Delta)^2}, \tag{21}$$

despite the discrete pulse profiles given by Eq. (18). Such a simple relation reveals that the linear chirp can be well controlled by engineering the dispersion profile for given T_0 and c_0. For example, for $c_0\,\mathrm{sgn}(D)\leqslant 0$, one can obtain asymptotically a vanishing linear chirp in constant dispersion or dispersion-increasing optical fibers, but a constant linear chirp in fibers with fast decreasing GVD.

It is worth noting that our HG solutions (18) involve only the dispersion and absorption profiles, regardless of the profile of nonlinearity. In other words, HG pulses arise from an interplay between strong dispersion and negligible nonlinearity, indicated by the parametric condition (15). Figure 2(a) shows the self-similar evolution of an initial, most simple HG pulse (or Gaussian) $\psi(0,\tau)=\exp(-0.5\tau^2)\exp(i\tau)$ propagating in an absorption medium but with two alternative nonlinearities. Figures 2(b) and 2(c) compare the numerical simulations at $z=200$ m for chirp and amplitude with our analytical results (20) and (21) as well as with the initial distribution. It is clearly seen that the pulse energy (width) decreases (increases) as the pulse propagates in such an absorption medium, with an exact scaling independent of the profile of nonlinearity. Besides, by other numerical simulations, we also confirm the self-similarities and the stabilities of the higher-order HG pulses, e.g., see one of those results

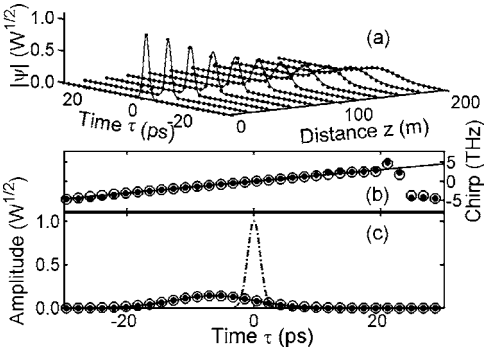

FIG. 2. (a) Evolution of an initial Gaussian pulse $\psi(0,\tau)=\exp(-0.5\tau^2)\exp(i\tau)$ in an absorption medium with the nonlinearity $\gamma(z)=\gamma_0\exp(-\epsilon z)$, where $\gamma_0=0.01\ \mathrm{W^{-1}\,m^{-1}}$ and $\epsilon=0.03$ (solid line), or $\gamma_0=-0.01\ \mathrm{W^{-1}\,m^{-1}}$ and $\epsilon=0.05$ (points). (b) and (c) compare the numerical simulations at $z=200$ m for chirp and amplitude [open circles for $\gamma(z)>0$ and solid circles for $\gamma(z)<0$] with the analytical results (solid line) as well as with the initial distribution (dash-dotted line). In both cases, $g(z)=-0.01\ \mathrm{m^{-1}}$ and $\beta(z)=\beta_0\exp(0.01z)$ with $\beta_0=0.01\ \mathrm{ps^2\,m^{-1}}$.

in Fig. 3, which is considered to show the evolution of an initial second-order HG pulse under the perturbations of the additive white noise [13].

Next, we point out that there exist the third novel type of localized self-similar solutions, called hybrid pulses, to Eq. (1) when η, μ, and ν are all constants. For our present purposes, it is essential that

$$\frac{\rho(z)}{E(z)}=\frac{\rho_0}{T_0E_0}T(z), \tag{22}$$

where the parameter $T(z)$ is given by Eqs. (16) and (19). Meanwhile, the phase offset $a(z)$ takes the same form as Eq. (17). With these parametric conditions, the function $F(\theta)$ in Eq. (8) can be determined definitely, though not easily, from

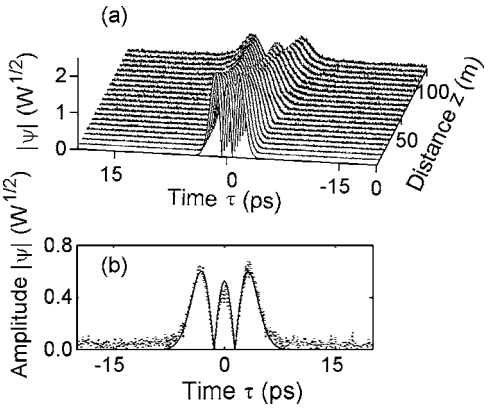

FIG. 3. (a) Evolution of an initial second-order HG pulse $\psi(0,\tau)=\exp(-0.5\tau^2)H_2(\tau)$ under the perturbations of the additive white noise with the noise intensity $5.0\times10^{-7}\ \mathrm{W\,m^{-2}}$. (b) compares the numerical simulation at $z=100$ m for the amplitude (dotted line) with the analytical result (18) (solid line). The model parameters are given by $\beta(z)=\beta_0\exp(0.01z)$, $\gamma(z)=\gamma_0\exp(-0.03z)$, and $g(z)=g_0$, where $\beta_0=0.01\ \mathrm{ps^2\,m^{-1}}$, $\gamma_0=0.01\ \mathrm{W^{-1}\,m^{-1}}$, and $g_0=-0.02\ \mathrm{m^{-1}}$.

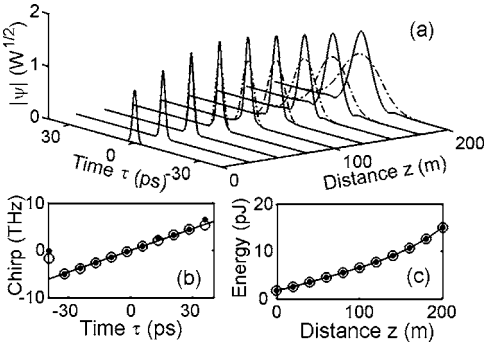

FIG. 4. (a) Evolution of an initial Gaussian pulse $\psi(0,\tau)=\exp(-0.5\tau^2)$ in the medium described by Eq. (22), subject to the nonlinearity $\gamma(z)=\gamma_0\exp(-0.01z)$ with $\gamma_0=0.01\ \mathrm{W^{-1}\,m^{-1}}$ (dash-dotted line), or with $\gamma_0=-0.01\ \mathrm{W^{-1}\,m^{-1}}$ (solid line). (b) and (c) compare the numerical simulations for the chirp and pulse energy [open circles for $\gamma(z)>0$ and solid circles for $\gamma(z)<0$] with the analytical results (solid line). In both cases, $\beta(z)=\beta_0\exp(0.01z)$ and $\beta_0=0.01\ \mathrm{ps^2\,m^{-1}}$.

the point of view of the ordinary differential equation. As is also evident in Eq. (8), this localized function has even or odd parity, depending on the value of the parameter ϕ (or n) and the initial pulse shapes. Significantly, we will see that the parity of this function enables us to look for the approximate analytical forms for our hybrid pulses within certain limits. As examples, we find in the limit $\theta\to\pm\infty$ that the profile takes the form $A(z,\tau)\propto\exp(-\frac{1}{2}\theta^2)H_n(\theta)$. But in the limit $\theta\to0$, the profile looks like some cnoidal forms according to the values of parameters ρ_0 and n. To be specific, for $\rho_0>0$, we have $A(z,\tau)\propto\mathrm{cd}(\theta/\vartheta,\ell)$ for even n or $A(z,\tau)\propto\mathrm{sn}(\theta/\vartheta,\ell)$ for odd n, where $\vartheta=\sqrt{(1+\ell^2)/2\phi}$ and $0<\ell<1$; whereas for $\rho_0<0$, we find $A(z,\tau)\propto\mathrm{cn}(\theta/\vartheta,\ell)$ for even n or $A(z,\tau)\propto\mathrm{sd}(\theta/\vartheta,\ell)$ for odd n, where $\vartheta=\sqrt{(1-2\ell^2)/2\phi}$ and $0<\ell<1/\sqrt{2}$. Obviously, these approximate predictions for hybrid pulses are applicable to all systems involving the parametric condition (22), and help to analyze the pulse characteristics qualitatively in these systems.

It should be emphasized, however, that in the system with exponentially decreasing or hyperbolically decreasing GVD, there also exist other exact asymptotic solutions $\psi(z,\tau)=\sqrt{E(z)}f(\tau)\exp(i\varpi D)$ by solving Eqs. (2) and (3) in the limit $z\to\infty$, where $f(\tau)$ is a temporal function proportional to sech, tanh, or some Jacobian elliptic functions subject to the values of parameters ϖ and ρ_0. As one can see, these solitonlike solutions are exactly chirp-free and are, in a broad sense, different from our hybrid self-similar pulses, which are always chirped linearly. Thus in this situation, to form the linearly chirped hybrid pulses, one should prepare elaborately the incident pulses with specific pulse profiles rather than with sech or tanh shapes.

Although no exact analytical forms exist for our hybrid self-similar solutions in terms of elementary functions, the pulse profiles and characteristics can be analyzed numerically. Figure 4(a) illustrates the evolution of an initial Gaussian pulse $\psi(0,\tau)=\exp(-0.5\tau^2)$ in the medium described by Eq. (22) [dash-dotted line, $\rho(z)>0$] and compares it with that involving the contrary nonlinearity [solid line, $\rho(z)<0$].

It is found that our hybrid pulses exist stably, although evolve distinctively, at both $\rho(z)>0$ and $\rho(z)<0$. Figures 4(b) and 4(c) exhibit the coincidence between the numerical simulations and our analytical results for the chirp and pulse energy. It is striking that a strictly linear chirp is maintained during propagation and the quantity $E(z)$ corresponds exactly to the energy of hybrid pulses. Also we find by numerical simulations that our hybrid pulses can be compressed under the condition $c_0\,\mathrm{sgn}(D)>0$ and the minimum pulse width takes place when the GVD-induced chirp cancels exactly the initial chirp.

We finally point out that the experimental realization is also possible for our three types of self-similar pulses by using the pulse characterization technique of frequency-resolved optical gating [7]. Generally, hybrid pulses are thought less operable in implementation than parabolic and HG ones for their more stringent condition (22). As one might expect, our work may open up other research opportunities for future experimental verification.

In summary, this is the first systematic study of the self-similar evolutions of parabolic, HG, and hybrid pulses applicable to the system described by the generalized NLS equation with varying coefficients. We demonstrate that parabolic pulses always occur in the regime of $\rho(z)>0$ under the parametric condition (11), and their self-similar evolutions are only determined by the input energy, not the initial pulse shapes. By contrast, HG and hybrid pulses can evolve stably in both regimes of $\rho(z)>0$ and $\rho(z)<0$, according to the corresponding parametric conditions (15) and (22). Besides, owing to the continuously enhanced linear chirp, parabolic pulses are monotonically broadened on propagation, but it is not always the case for HG and hybrid pulses. Under appropriate initial conditions, the latter two will go through an initial pulse narrowing stage when the GVD induces a chirp in opposition to the initial chirp. We show further the major discrepancies between HG and hybrid pulses according to which role the nonlinearity plays during the pulse evolution. It is demonstrated that the nonlinearity always plays a very minor role in HG pulse propagation, but a rather major role in the formation of hybrid pulses.

Despite these fascinating, intrinsic characteristics, our self-similar pulses exhibit many universal features by virtue of which one can achieve directly the well-defined linearly chirped output pulses from an optical fiber, an amplifier, or an absorption medium, under appropriate parametric conditions. As one could envision, these newly found pulses may find significant applications.

S.C. acknowledges the support from NSF-China. D.-S.G. is supported in part by 973 project of China.

[1] G. I. Barenblatt, *Scaling, Self-Similarity, and Intermediate Asymptotics* (Cambridge University Press, Cambridge, England, 1996).
[2] C. R. Menyuk, D. Levi, and P. Winternitz, Phys. Rev. Lett. **69**, 3048 (1992).
[3] T. M. Monro, D. Moss, M. Bazylenko, C. Martin de Sterke, and L. Poladian, Phys. Rev. Lett. **80**, 4072 (1998); T. M. Monro, P. D. Millar, L. Poladian, and C. M. de Sterke, Opt. Lett. **23**, 268 (1998).
[4] M. Soljacic, M. Segev, and C. R. Menyuk, Phys. Rev. E **61**, R1048 (2000).
[5] K. D. Moll, A. L. Gaeta, and G. Fibich, Phys. Rev. Lett. **90**, 203902 (2003).
[6] D. Anderson, M. Desaix, M. Karlsson, M. Lisak, and M. L. Quiroga-Teixeiro, J. Opt. Soc. Am. B **10**, 1185 (1993).
[7] M. E. Fermann, V. I. Kruglov, B. C. Thomsen, J. M. Dudley, and J. D. Harvey, Phys. Rev. Lett. **84**, 6010 (2000); V. I. Kruglov, A. C. Peacock, J. M. Dudley, and J. D. Harvey, Opt. Lett. **25**, 1753 (2000).
[8] T. Hirooka and M. Nakazawa, Opt. Lett. **29**, 498 (2004).
[9] F. Ö. Ilday, J. R. Buckley, W. G. Clark, and F. W. Wise, Phys. Rev. Lett. **92**, 213902 (2004).
[10] V. I. Kruglov, A. C. Peacock, and J. D. Harvey, Phys. Rev. Lett. **90**, 113902 (2003).
[11] V. N. Serkin, and A. Hasegawa, Phys. Rev. Lett. **85**, 4502 (2000); V. N. Serkin, A. Hasegawa, and T. L. Belyaeva, *ibid.* **92**, 199401 (2004).
[12] S. Chen and L. Yi, Phys. Rev. E **71**, 016606 (2005).
[13] S. Chen, D. Shi, and L. Yi, Phys. Rev. E **69**, 046602 (2004).
[14] M. Abramowitz and I. A. Stegun, *Handbook of Mathematical Functions* (National Bureau of Standards, Dover, New York, 1972).